Striving for Small-Signal Stability

Loop-Based and Device-Based Algorithms for Stability Analysis of Linear Analog Circuits in the Frequency Domain

By Michael Tian, V. Visvanathan, Jeffrey Hantgan, and Kenneth Kundert

Negative feedback techniques are widely used in analog and RF design to improve circuit properties such as variation tolerance, bandwidth, impedance matching, and output waveform distortion. In practice, unwanted local return loops also exist around individual transistors through parasitic capacitance. As the size of transistors continues to shrink and the bandwidth of transistors continues to broaden, these local return loops degrade circuit performance significantly in the high-frequency regime. Stability is always a serious concern for feedback circuits. Self-oscillations have been found above and/or beyond the bandwidth in such diversified circuits as optical fiber system receivers, power amplifiers, and distributed microwave amplifiers. It is critical to evaluate stability and stability margin of a feedback circuit. Such information can be used for optimization in the early design stage and for diagnosis in physical realization stage.

Single-loop theory/multiloop reality is the state-of-the-art of stability analysis [8]. All physical networks in the frequency band of interest are intrinsically multiloop structures, yet it is still common practice to assess stability from single-loop theory. In this article, based on Bode's definition of return ratio with respect to a single controlled source, the loop-based two-port algorithm and device-based gain-nulling algorithm are proposed for small-signal stability analysis. These two algorithms are complementary in terms of applicability, and they produce accurate stability information for single-loop networks. After a brief primer on feedback and stability, we review Bode's feedback theory, where the return difference and return ratio concepts are applicable to general feedback configurations and avoid the necessity of identifying μ and β. Middlebrook's null double-injection technique, which provides a laboratory-based way to measure return ratio, is then discussed in the modern circuit analysis context. We then extend the unilateral feedback model used in Middlebrook's approach to accommodate both normal- and reverse-loop transmission and characterize the return loop using a general two-port analysis. This loop-based two-port algorithm determines the stability of a feedback network in which a critical wire can be located to break all return loops. The device-based gain-nulling algorithm is then discussed to evaluate the influence of the local return loops upon network stability. This algorithm determines the stability of a feedback network in which a controlled source can be nulled to render the network to be passive. Conditions under which these two algorithms can be applied are discussed, and numerical results are provided.

The Feedback-Stability Relationship

To illustrate the relation between feedback and stability, the ideal single-loop feedback network is shown in Fig. 1. Following the terminology of [6], μ represents the transfer function of the unilateral forward active path and is usually referred to as an *open-loop transfer function*, while β represents the transfer function of a unilateral feedback path. The presence of the ideal adder in the diagram indicates there is no loading effect at the input. Under these assumptions, it is easily shown that the overall transfer function, which is often called a *closed-loop transfer function*, is given by

$$A = \frac{s_o}{s_i} = \frac{\mu}{1 - \mu\beta} , \tag{1}$$

where $1 - \mu\beta$ is referred to as the *feedback factor*. Under the condition $1 - \mu\beta = 0$, a feedback network will function like an oscilla-

tor. This condition is known as the *Barkhausen criterion* [2], which states that the frequency of a linear(ized) oscillator is determined by the condition that the phase shift of $\mu\beta$ is zero provided that the magnitude of $\mu\beta$ equals

> All physical networks in the frequency band of interest are intrinsically multiloop structures, yet it is still common practice to assess stability from single-loop theory.

unity. The linear oscillator design should ensure that this criterion is satisfied, while the amplifier design should ensure that the circuit operates away from this critical point. Stability margin is defined as the distance between $\mu\beta$ and unity.

The zeros of the feedback factor are the natural frequencies (poles) of the network. However, pole-zero analysis is not preferred for studying stability not only because it has numerical difficulties with large networks but also because it does not provide stability margin that is of paramount interest to circuit designers. Since input s_i and output s_o can be either current or voltage, feedback networks often can be classified into four different configurations [3]: *shunt-shunt*, *shunt-series*, *series-shunt*, and *series-series*. The *input-output two-port approach* [3, 6, 7] models these four configurations using Y, G, H, and Z parameter-based two-port analysis. Symbolic expressions of loop gain $\mu\beta$ in terms of these parameters are therefore derived to provide stability information.

It should be noted that the ideal single-loop feedback network shown in Fig. 1 is not an adequate representation of a practical feedback network. In practice, the active path may not be strictly unilateral; the feedback path is usually bilateral, and the input and output coupling networks are often complicated. A general feedback configuration containing an input coupling and an output coupling network is shown in Fig. 2. In addition, as pointed out in [6], not every single-loop feedback network can be classified as being in one of these four configurations. It is also important to know that loop gain (the stability measure of a re-

1. The ideal single-loop feedback network.

2. A general feedback network with input and output coupling [6].

turn loop) is uniquely determined by the loop parameters—it should not vary as the type and location of input source changes. However, since network zeros enter the calculation of loop gain $\mu\beta$, input-output two-port analysis produces inconsistent stability information that does depend upon the type and location of input source [4]. Thus, a general and more accurate approach to perform stability analysis is desirable.

Bode's Feedback Theory

Bode's original theory was published in [1] and was later extended in [6]. In a general feedback network, the quantity of crucial effect upon the network stability is the controlled source of the amplifier. Without loss of generality, we assume this source is a *voltage-controlled current source* specified as $i = xv$. In the subsequent discussion, x refers to this controlled source. The definition of return difference is given below.

Definition 1 [6]. The return difference $F(x)$ of a feedback network with respect to a controlled source x is said to be the ratio of two functional values assumed by network determinant under (a) the condition that x assumes its nominal value, and (b) the condition that x assumes the value zero:

$$F(x) = \frac{\Delta}{\Delta\big|_{x=0}}. \tag{2}$$

Return difference $F(x)$ is the most important quantity encountered in feedback theory for a number of practical reasons. First, stability of the network depends upon the zeros of $F(x)$ in the complex frequency plane, which are natural frequencies of the network. Second, $F(x)$ is considered as a generalization of the feedback factor $1 - \mu\beta$ in the ideal feedback network shown in Fig. 1. Third, the sensitivity function $S(x)$ of the amplifier with respect to the element x is closely related to the return difference $F(x)$—and in many practical cases, $S(x)$ is approximately equal to the reciprocal of return difference.

Return ratio $T(x)$ is defined as

$$T(x) = F(x) - 1 = \frac{\Delta - \Delta\big|_{x=0}}{\Delta\big|_{x=0}}. \tag{3}$$

In the engineering context, the negative of return ratio $T(x)$ is referred to as *loop gain*, which is also a generalization of $\mu\beta$ in the ideal single-loop feedback network shown in Fig. 1. Correspondingly, the Barkhausen criterion in terms of return difference and return ratio is $F(x) = 0$ and $T(x) = -1$, respectively.

Referring to Fig. 3, return difference and return ratio can be physically interpreted as follows. First, deactivate all network input $i_1, \ldots, i_N$; second, replace the input of controlled source x with an external voltage source of 1 V, thus x no longer depends
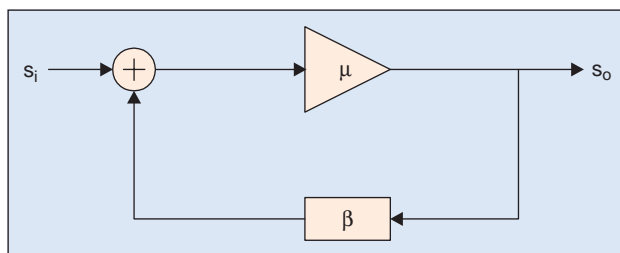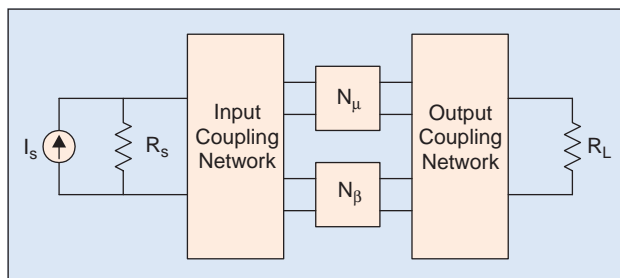
upon v_i. This 1 V input produces a current of x amperes at the output of the controlled source. The transmitted voltage to the original input of the controlled source (v_i) is then the negative of the return ratio $T(x)$. Also, the return difference $F(x)$ is simply the difference between the excitation of 1 V applied at the input of the controlled source and the transmitted voltage to the original input of the controlled source. From the *proportionality property* of a linear circuit, the return ratio is simply $-v_i / v_{ext}$ in case the external source v_{ext} is not 1 V. The physical interpretation of return ratio $T(x)$ is important because it is upon this interpretation that Middlebrook based the laboratory-oriented measurement technique to obtain the return ratio of a feedback network.

For the subsequent discussion, we consider the special case that the controlled source of interest is a one-port element. Instead of relating a voltage and a current at different ports, x relates the voltage and current at the same port. The definition of return difference and return ratio can still be used. The original circuit equation is

$$\begin{bmatrix} & \vdots & \\ \cdots & Y_{jj} & \cdots \\ & \vdots & \end{bmatrix} \begin{bmatrix} \vdots \\ v_j \\ \vdots \end{bmatrix} = \begin{bmatrix} \vdots \\ i_j \\ \vdots \end{bmatrix}, \tag{4}$$

where the determinant of circuit matrix is Δ.

Now we replace the one-port element by an independent current source of x amperes. Meanwhile, we remove all network excitations, and then the circuit equation becomes

$$\begin{bmatrix} & \vdots & \\ \cdots & Y_{jj} - x & \cdots \\ & \vdots & \end{bmatrix} \begin{bmatrix} \vdots \\ \widetilde{v}_j \\ \vdots \end{bmatrix} = \begin{bmatrix} 0 \\ -x \\ 0 \end{bmatrix}, \tag{5}$$

where the determinant of circuit matrix now is $\Delta|_{x=0}$, and the response $\widetilde{v}_j$ due to the current excitation x is simply

$$\widetilde{v}_j = -x \frac{\Delta_{jj}}{\Delta|_{x=0}}, \tag{6}$$

where Δ_{jj} is the co-factor of the Y_{jj} term.

Since $\widetilde{v}_j$ is the voltage response due to the current source x at the same port, then

$$\frac{\widetilde{v}_j}{-x} = \frac{\Delta_{jj}}{\Delta|_{x=0}} = \frac{1}{Y}, \tag{7}$$

where Y is the admittance of the one-port network that x faces. Return ratio $T(x)$ for a one-port element x is then given by

Null double injection has been widely applied in both laboratory-based measurement and circuit analysis.

$$T(x) = -\widetilde{v}_j = \frac{x}{Y}. \tag{8}$$

This equation will be used in the subsequent sections for the development of return-loop models.

Stability margin is defined as the distance between return ratio and –1, or equivalently, the distance between loop gain and unity. Note that the return ratio is a complex function of frequency. For the completeness of the feedback theory, the definitions of gain margin and phase margin are given below.

Definition 2 [6]. The gain margin is defined to be the amount of magnitude in decibels of the return ratio below the 0 dB level at the frequency for which the phase is –180 degrees.

Definition 3 [6]. The phase margin is defined to be the phase difference in degrees of the return ratio above –180 degrees at the frequency for which the gain is 0 dB.

Null Double-Injection Technique

In his original work [9], Middlebrook proposed the so-called *null double-injection* technique to measure return ratio based on its physical interpretation. In this section, we review this approach in the modern circuit analysis context.

Recalling the physical interpretation of return ratio in the last section, it involves deactivating network input and breaking the controlled source at the input side. This *breakpoint* concept can be extended, without loss of accuracy, to break the feedback loop at any location on either the active path or the feedback path, as long as the dc impedance characteristics are not disturbed. To demonstrate this concept, the signal flow graph of a broken feedback loop is illustrated in Fig. 4.

By assuming the feedback loop has unilateral signal flow from e to f, without loss of generality, we can model the whole feedback loop with an impedance on the input side and a controlled source with an impedance on the output side in either of the two configurations (essentially, *Norton equivalent* and *Thévenin equivalent*) shown in Fig. 5. Both configurations model the same loop, thus constants k_1 and k_2 must satisfy $k_1 = -k_2 Y_e Y_f$. s_e and s_f must be of the same physical quantities, so the return ratio is either $-v_f / v_e$ or $-i_f / i_e$.

If we view the return ratio as the voltage ratio $-v_f / v_e$, we can substitute the representation of Fig. 5(a) into the feedback loop
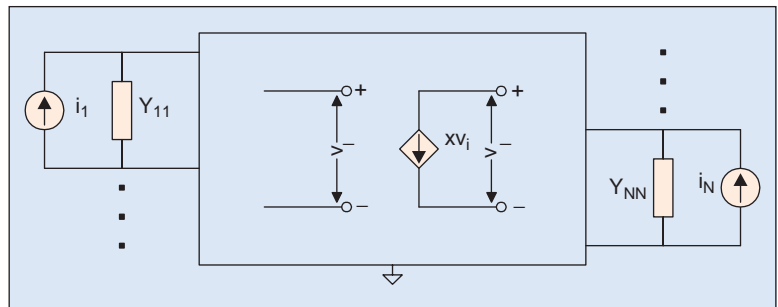
3. The physical interpretation of return difference and return ratio.

in Fig. 4. At the output side of the feedback loop, note that the network is loaded with Y_e since the dc bias of the original circuit is not disturbed, we have
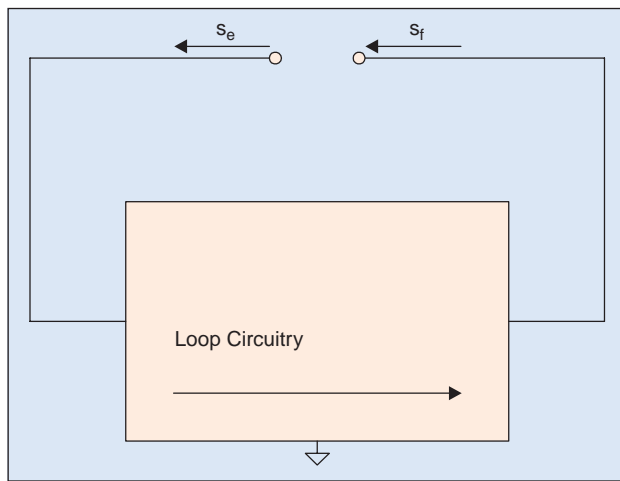
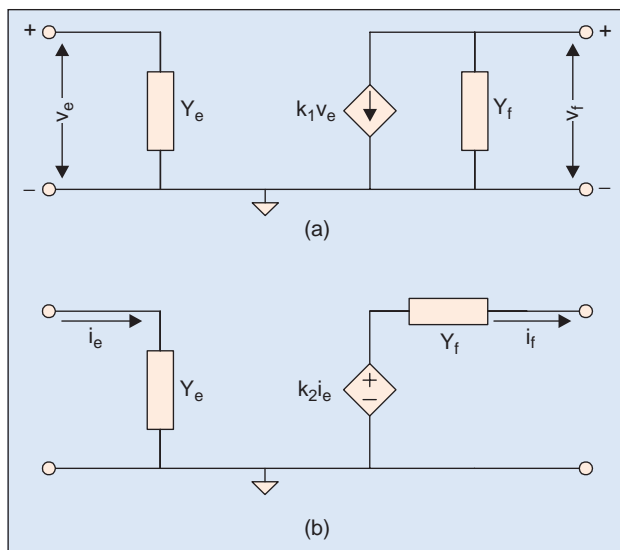$$k_1 v_e + \frac{v_f}{Y_e + Y_f} = 0,$$ (9)

thus the return ratio is

$$T = -\frac{v_f}{v_e} = \frac{k_1}{Y_e + Y_f}.$$ (10)

Going back to the alternative view of the return ratio as a system that has currents as its input and output signals, we plug in the representation of Fig. 5(b) into the feedback loop in Fig. 4 and have the following equation:

$$k_2 i_e = \left(\frac{1}{Y_e} + \frac{1}{Y_f}\right) i_f.$$ (11)

4. The signal flow graph of a broken feedback loop.

5. The Norton and Thévenin equivalents of the feedback loop.

Based on the relation between k_1 and k_2, we conclude once again that

$$T = -\frac{i_f}{i_e} = \frac{k_1}{Y_e + Y_f}.$$ (12)

We can also make use of Eq. (8). At the normal circuit operation, node e and f are connected together, thus Fig. 5(a) is equivalent to a one-port element (discussed in the previous section) with $x = k_1$ and $Y = Y_e + Y_f$. Directly following Eq. (8), we have

$$T = \frac{x}{Y} = \frac{k_1}{Y_e + Y_f}.$$ (13)

Figure 5 is the fundamental return-loop model used in Middlebrook's approach, and Eq. (13) is the essential formula to calculate the return ratio under this model.

To analyze the stability of the feedback loop, it does not matter whether the designer views voltage or current as the signal of interest; both produce the same answer, as long as the dc impedances are not disturbed when the loop is broken. In practice, this requires careful selection of the break-point location. For the voltage driving case, the break point should be located where the impedance Y_f looking *backward* from the break point is sufficiently smaller than the impedance Y_e looking *forward* from the break point; the opposite condition, $Y_f \ll Y_e$ is necessary for the current driving case to give a correct result. Generally, for an actual network, it may not be possible to find a break point that satisfies either of these extreme conditions.

By performing two signal-injection-based return ratio measurements, the influence of break point on dc impedance can be canceled out such that the location of the break point can be selected anywhere on the loop. This double-injection configuration is shown in Fig. 6. At the normal circuit operation, both i_{inj} and v_{inj} are set to zero; thus, the loop properties are undisturbed.

For the first signal injection, i_{inj} and v_{inj} are provided simultaneously to null i_f. We have the following equation at the output side of the feedback loop:

$$k_1 v_e + Y_f v_f = 0,$$ (14)

and the *null voltage return ratio* T_v^n is defined and calculated as

$$T_v^n = -\frac{v_f}{v_e}\bigg|_{i_f=0} = \frac{k_1}{Y_f}.$$ (15)

For the second signal injection, i_{inj} and v_{inj} are provided simultaneously to null v_f. We have the following equation at the output side of the feedback loop:

$$-i_f = k_1 \frac{i_e}{Y_e},$$ (16)

and the *null current return ratio* T_i^n is defined and calculated as

$$T_i^n = -\left.\frac{i_f}{i_e}\right|_{v_f=0} = \frac{k_1}{Y_e}. \tag{17}$$

According to Eq. (13) and manipulating the algebra, we have the return ratio

$$T = \frac{T_v^n T_i^n}{T_v^n + T_i^n}, \tag{18}$$

and

$$\frac{Y_f}{Y_e} = \frac{T_i^n}{T_v^n}. \tag{19}$$

Compared with other double-injection techniques, null double injection is numerically stable even when return ratio T approaches zero. Today, this technique has been widely applied in both laboratory- based measurement and circuit analysis.

Evaluation of True Return Ratio

The return-loop model used in Middlebrook's approach implicitly assumes that signals flow through the feedback loop unilaterally. This is a reasonable assumption for most low-frequency applications. However, as we pointed out before, for most practical designs, the active path may not be strictly unilateral, and the feedback path is usually bilateral. Thus, in addition to *normal loop transmission*, *reverse loop transmission* also exists around the feedback loop. The signal level of reverse transmission, which is ignored by the null double-injection technique and most other approaches, can be as large as normal transmission for microwave applications [8]. To accurately evaluate the stability of a feedback network, both normal- and reverse-loop transmission should be considered. In this section, we extend the unilateral return-loop model shown in Fig. 5 to the bilateral return-loop model, and we calculate the *true return ratio,* which is proven to be the sum of *normal return ratio* and *reverse return ratio.*

Figure 7 shows the bilateral return-loop model configured for the double-injection technique. Recalling that at the normal circuit operation i_e equals to i_f and v_e equals v_f, Y_e, Y_f, k_1, and k_3 are connected in parallel. Compared with the one-port case discussed above, we know that $x = k_1 + k_3$, $Y = Y_e + Y_f$; then, for the bilateral model, we have

$$T = \frac{x}{Y} = \frac{k_1 + k_3}{Y_e + Y_f}. \tag{20}$$

The bilateral return-loop model can be characterized using a general two-port analysis. Let i_{inj} and v_{inj} be the driving (input) signals and i_f and v_e be the dependent (output) signals. Since the feedback network is linear, the only constraint to be placed upon each dependent signal, by superposition, is the linear sum of the two values it would have due to each input signal alone. Thus

$$\begin{bmatrix} i_f \\ v_e \end{bmatrix} = \begin{bmatrix} A & B \\ C & D \end{bmatrix} \begin{bmatrix} i_{inj} \\ v_{inj} \end{bmatrix}. \tag{21}$$

The A, B, C, and D parameters are characterized by a double-injection technique that is essentially two small-signal ac analyses: for the first small-signal ac analysis, we set $i_{inj} = 0$ and $v_{inj} = 1$, then

$$B = \left.i_f\right|_{i_{inj}=0,\,v_{inj}=1} \quad \text{and} \quad D = \left.v_e\right|_{i_{inj}=0,\,v_{inj}=1}; \tag{22}$$
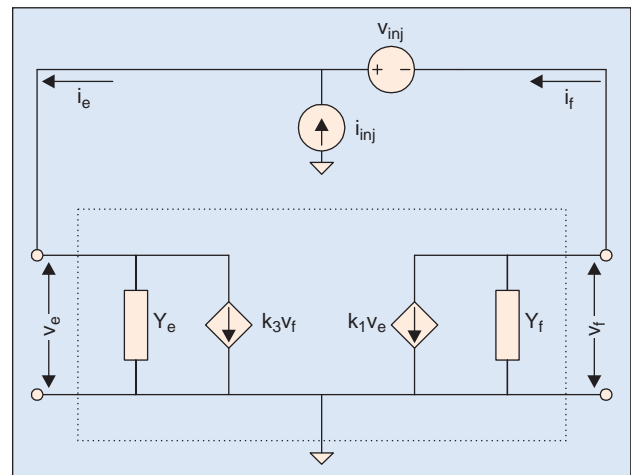
for the second small-signal ac analysis, we set $i_{inj} = 1$ and $v_{inj} = 0$, then

$$A = \left.i_f\right|_{i_{inj}=1,\,v_{inj}=0} \quad \text{and} \quad C = \left.v_e\right|_{i_{inj}=1,\,v_{inj}=0}. \tag{23}$$

Here the double-injection technique is performed to characterize the return loop. Although a similar technique is used in
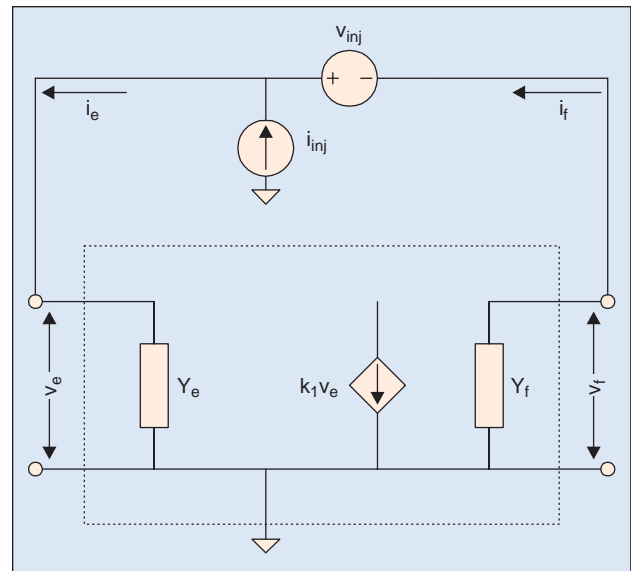
6. The illustration of double-injection technique.

7. Double-injection technique based on the bilateral return loop model.

Middlebrook's approach, the purpose there is to calculate the voltage and current return ratios.

Once the return loop is characterized, the relationship between the k_1, k_3, Y_e, Y_f, and A, B, C, D parameters needs to be derived. Considering Fig. 7, circuit equations at the input side and output side of the feedback loop are

$$-Y_e v_e + i_{\text{inj}} + i_f - k_3 (v_e - v_{\text{inj}}) = 0, \qquad (24)$$

$$k_1 v_e + i_f + Y_f (v_e - v_{\text{inj}}) = 0 . \qquad (25)$$

Compared with Eq. (21), we have the expressions for A, B, C, and D in terms of k_1, k_3, Y_e, and Y_f:

$$A = \frac{-k_1 - Y_f}{k_1 + k_3 + Y_e + Y_f}, \qquad B = \frac{Y_e Y_f - k_1 k_3}{k_1 + k_3 + Y_e + Y_f},$$

$$C = \frac{1}{k_1 + k_3 + Y_e + Y_f}, \qquad D = \frac{k_3 + Y_f}{k_1 + k_3 + Y_e + Y_f}.$$

Solving these four equations, we have

$$k_1 = \frac{AD - BC - A}{C}, \qquad (26)$$

$$k_3 = \frac{AD - BC + D}{C}, \qquad (27)$$

$$Y_e = \frac{1 - AD + BC + A - D}{C}, \qquad (28)$$

$$Y_f = \frac{BC - AD}{C}. \qquad (29)$$

Replacing Eqs. (26), (27), (28), and (29) into Eq. (20), the formula that accurately calculates the true return ratio is

$$T = \frac{2(AD - BC) - A + D}{2(BC - AD) + A - D + 1}. \qquad (30)$$

Recalling that the only difference between the unilateral model and the bilateral model is that the unilateral model ignores the reverse transmission factor k_3, by replacing Eqs. (26), (28), and (29) into Eq. (13), the null double-injection technique calculates the normal return ratio as

$$T_{\text{normal}} = \frac{AD - BC - A}{2(BC - AD) + A - D + 1} . \qquad (31)$$
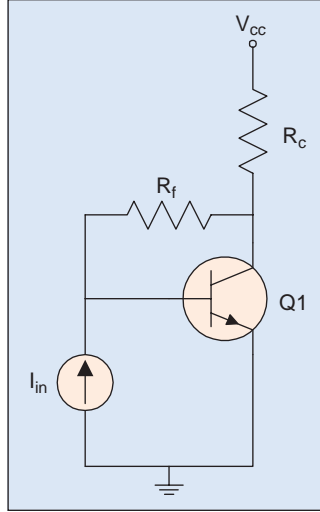
8. A simple bipolar feedback circuit.

Accordingly, by ignoring k_1, the reverse return ratio is calculated as

$$T_{\text{reverse}} = \frac{AD - BC + D}{2(BC - AD) + A - D + 1} . \qquad (32)$$

It is obvious that the true return ratio is the sum of normal return ratio and reverse return ratio.

The evaluation of Eq. (30) is referred to as a *loop-based two-port algorithm* in this article. In summary, this algorithm consists of two steps. First, deactivate the network input and perform two small-signal ac analyses to characterize the A, B, C, and D parameters; then the true return ratio is calculated using Eq. (30). This loop-based algorithm applies definitely to a single-loop feedback network and a multiloop feedback network in which a critical wire can be located to break all return loops. In the multiloop case, model parameter k_1, k_3, Y_e, and Y_f are lumped from all return loops.

It should be pointed out the proposed loop-based two-port algorithm differs fundamentally from the input-output two-port analysis described in [3, 6, 7]. The latter approach models the whole feedback network using two-port analysis based on the ideal single-loop feedback network shown in Fig. 1. Both the input and output of the feedback network can be either current or voltage, thus the specific feedback configuration needs to be pre-identified to perform input-output two-port analysis. While our loop-based two-port algorithm only models the feedback loop and its associated loading effects, all feedback networks fall into the same loop model; since the driving signal and return signal are of the same physical quantity, the voltage case and current case are essentially equivalent. Furthermore, the loop model in our approach is purely determined from the loop parameters, which provides a unique stability measure, while input-output two-port analysis produces results dependent upon the type and location of network input [4]. This is highlighted by a detailed example in the Numerical Results section.

The Device-Based Gain-Nulling Algorithm

Our loop-based two-port algorithm requires that circuit designers have access to the return loop, such that a break point can be placed to characterize the loop. There are two categories of applications that are of much interest to microwave circuit designers. In the RF regime, the device parasitic effect becomes significant. Take the MOSFET transistor as an example: the signal flows back from the internal drain to the internal gate through parasitic capacitance C_{gd}. Under this scenario, the *local return loop* exists around an individual transistor. *Self-oscillation* is a frequently encountered phenomenon in high-frequency design, so it is very important to evaluate the stability of an individual transistor. In this case, one design objective is to ensure that an individual transistor is stable with a reasonable stability margin beyond the operating bandwidth. On the other hand, the objective of linear

oscillator design is to ensure the return ratio goes through the critical oscillating point (Barkhausen criterion) at the desired frequency. Some oscillators depend on the internal local loops alone to start, others require an external loop or sometimes a trigger is needed. In all cases, return ratio is a useful design and analysis tool. However, since the feedback loop is hidden inside the device, our loop-based algorithm can no longer be applied to these types of applications.

To address this issue, let us go back to the original definition of return difference and return ratio. There are two factors that prohibit the direct use of them in practice. First, direct measurement of a network determinant is almost impossible; second, the original definition is based on a single controlled source, while the actual return loops are far more complicated. Our loop-based algorithm lumps the complicated loop structure into the bilateral return loop model.

In circuit analysis, the calculation of the network determinant is rather simple. Given an $N \times N$ matrix A, after LU decomposition, we have

$$A = L \times U, \tag{33}$$

where L is the lower triangular with all diagonal elements equal to one, and U is the upper triangular. The determinant function of A is simply

$$\Delta = \prod_{i=1}^{N} U_{ii}. \tag{34}$$

Numerically, the determinant of a large matrix can be off the limit of the floating-point representation. One way to handle this problem is to order the diagonal elements before the return ratio computation, that is

$$T(x) = \frac{\prod_{i=1}^{N} U_{ii}}{\prod_{i=1}^{N} U_{ii}^0} - 1 = \prod_{i=1}^{N} \frac{\widetilde{U}_{ii}}{\widetilde{U}_{ii}^0} - 1, \tag{35}$$

where $\widetilde{U}_{ii}$ and $\widetilde{U}_{ii}^0$ are ordered to be monotonically increasing or monotonically decreasing. This should always work since the return ratio $T(x)$ itself has a reasonable value.
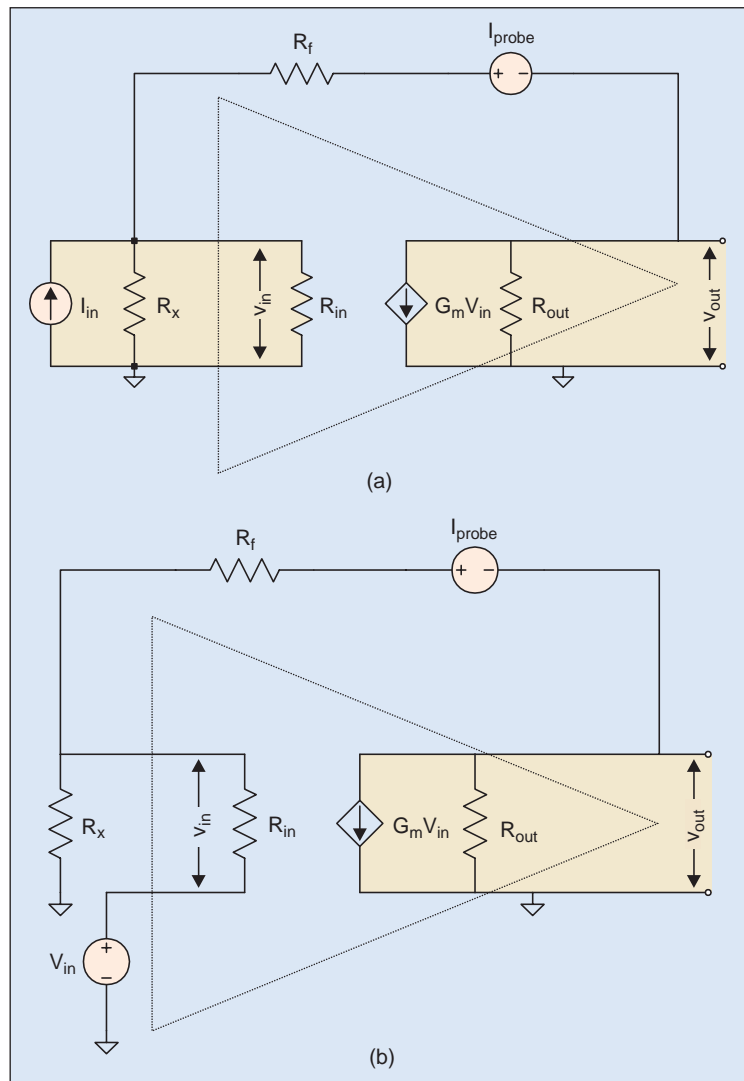
Although the single-controlled-source-based definition cannot be applied to a general sophisticated feedback network, the determinant-based return ratio calculation can be perfectly applied to assess the stability of an individual transistor with local return loops. This approach, referred to as a *device-based gain-nulling algorithm*, calculates return ratio based on individual transistors at each frequency: the normal network determinant and the network determinant with controlled source x nulled are first calculated, then the return ratio associated with this specific transistor is determined by Eq. (3). Here, the

controlled source x is assumed to be the dominant controlled source (g_m in most cases) in the transistor under investigation. Unlike our loop-based algorithm, the gain-nulling algorithm is device-based, and there is no need to access the return loop.
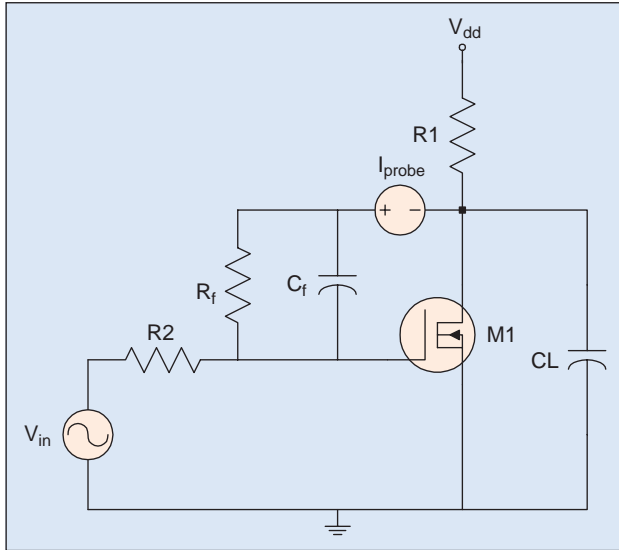
Applicability of Loop-Based and Device-Based Algorithms

The loop-based two-port algorithm produces stability information for a specific return loop, while the device-based gain-nulling algorithm produces stability information for a specific controlled source. Before proceeding further, we should first investigate the condition under which these two algorithms produce consistent stability information for a single-loop feedback network.

Our loop-based and device-based algorithms produce consistent stability information for a single-loop feedback network as long as the following condition is satisfied: *all controlled sources of the network appear in the network determinant in a simple product form* [6]. This implies the nulling of any controlled

9. A single-loop feedback circuit, $R_x = 200\,\mathrm{k}$, $R_f = 100\,\mathrm{k}$, $R_{in} = 50\,\mathrm{k}$, $R_{out} = 1\,M$, $g_m = 1\,m$.

10. A single MOSFET feedback circuit.

2. If the reverse transmission can be ignored, only the device-based algorithm produces accurate stability information for the network. If the network is a multiloop network, the loop-based algorithm can no longer be applied since no wire can be found to break both global and local loops.
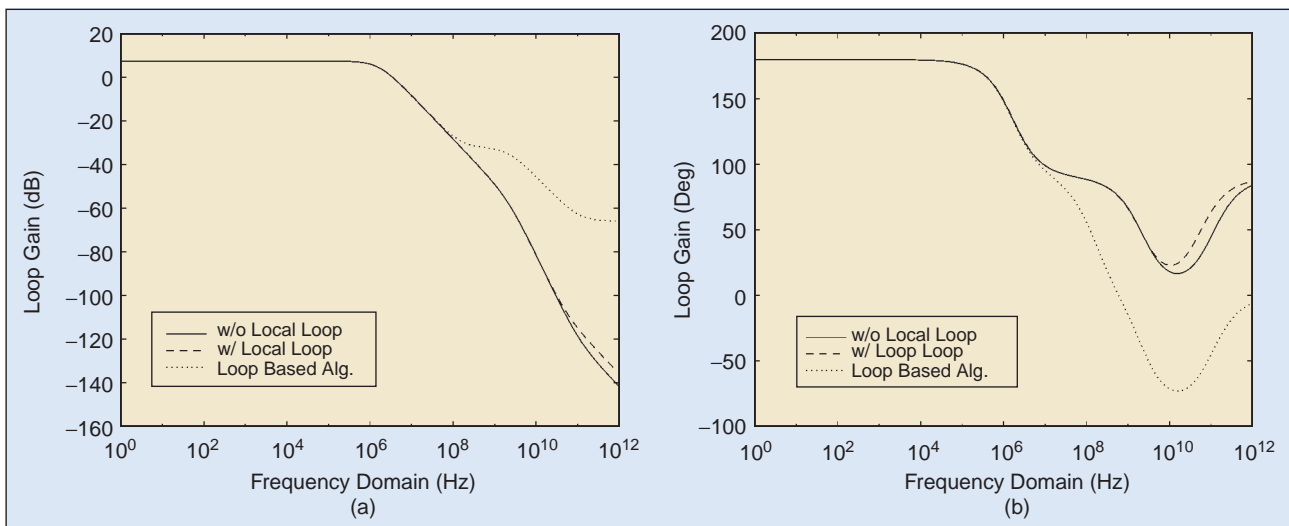
3. If the local return loop can be ignored, only the loop-based algorithm produces accurate stability information for the network. The loop-based algorithm produces accurate stability information for a multiloop network as long as a critical wire can be found to break all loops. Nulling the normal transmission-controlled source does not render the whole network to be passive, thus the device-based algorithm cannot be applied

4. If none of these two factors can be ignored, this corresponds to general multiloop networks. Neither our loop-based nor our device-based algorithms can be applied.

It is obvious that our loop-based and device-based algorithms are complementary in terms of applicability for single-loop networks. When the local return loop is the only feedback loop in the network, the loop-based algorithm can no longer be applied, and our device-based algorithm produces accurate stability information. When the single-loop network consists of multiple controlled sources, and they are not in the single product form in network determinant, our loop-based algorithm produces accurate stability information since a wire can always be found under this multiple device situation. Case 2 and Case 3 are the exact conditions under which our loop-based and device-based algorithms can be applied to multiloop applications.

Numerical Results

The proposed loop-based two-port algorithm and device-based gain-nulling algorithm have been implemented in a Spectre circuit simulator. In this section, numerical results are given to illustrate the accuracy advantage over input-output two-port analysis and the null double-injection technique. The conditions under which our loop-based and device-based algorithms can be applied to multiloop applications are also demonstrated with real circuit designs. Although return ratio has been used through the theoretical

source in the network renders the whole network to be passive. In other words, the return ratio with respect to any controlled source is the same.

This condition can be further extended to multiloop cases: for a feedback network that consists of multiple loops, if a critical controlled source can be located such that the nulling of this source renders the whole network passive, return ratio with respect to this controlled source is the accurate stability measure of the network.

A simple circuit shown in Fig. 8 can be used to illustrate the applicability of our loop-based and device-based algorithms. Two factors affect the applicability of this circuit: the local return loop inside the transistor and the reverse-loop transmission around the return loop. There are four cases:

1. If both the local loop and reverse transmission can be ignored, both our loop-based and device-based algorithms produce accurate and consistent stability information for the network.

11. The loop-gain waveform of the single MOSFET circuit.

development in previous sections, loop gain—the negative of return ratio and widely used in the engineering context—has been produced as the output of stability analysis.

Our loop-based and device-based algorithms are complementary in terms of applicability for single-loop networks.

Single-Loop Feedback Circuit

This example is taken from [4] and is used to demonstrate the consistency between our loop-based two-port algorithm and the device-based gain-nulling algorithm. Our loop-based and device-based algorithms produce consistent loop-gain results for single-loop circuits and do not depend upon the type and location of input sources. In contrast, input-output two-port analysis, which does depend upon the type and location of input sources, could produce yet another loop-gain result.

The circuit diagram is shown in Fig. 9. Note that the circuits in Fig. 9(a) and Fig. 9(b) are exactly the same except the type and location of the input source is different. Figure 9(a) shows a shunt-shunt feedback configuration, while Fig. 9(b) shows a series-shunt feedback configuration.

This circuit contains a single return loop and a single controlled source, and it corresponds to Case 1 discussed above. Current probe I_{probe} (equivalent to the zero-valued voltage source in Spectre) is inserted into the return loop to characterize the loop. I_{probe} is used to add v_{inj} and i_{inj} on-the-fly for two-port analysis. As expected, both our loop-based and device-based algorithms produce the same loop-gain result of 35.09 for either the shunt-shunt or series-shunt configurations.

In contrast, the input-output two-port analysis produces a loop-gain result of 25.71 for the shunt-shunt configuration and 66.85 for the series-shunt configuration [4]. Note that these two numbers differ by more than a factor of two. This observation demonstrates that even for a typical single-loop circuit, input-output two-port analysis produces inconsistent loop-gain results as the type and location of the input source changes.

The difference of loop-gain results between our algorithms and input-output two-port analysis can be explained as that the input-output two-port analysis is purely based on the simplified unidirectional feedback model. For this circuit, the active path is strictly unidirectional, while the feedback path is not.

Single MOSFET Feedback Circuit

Figure 10 shows a single MOSFET feedback circuit that is used to illustrate the stability analysis of a feedback circuit operating at such a high frequency that the local return loops cannot be neglected.

For a MOSFET transistor, local return loops exist between the drain and gate through parasitic capacitances. As frequency
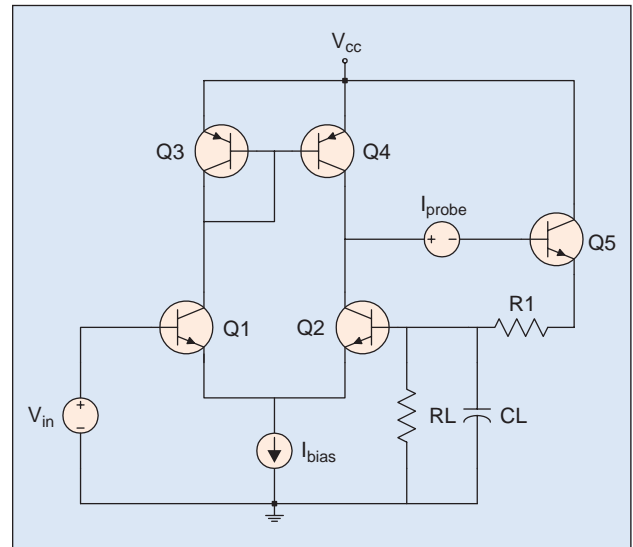

12. A bipolar operational amplifier.
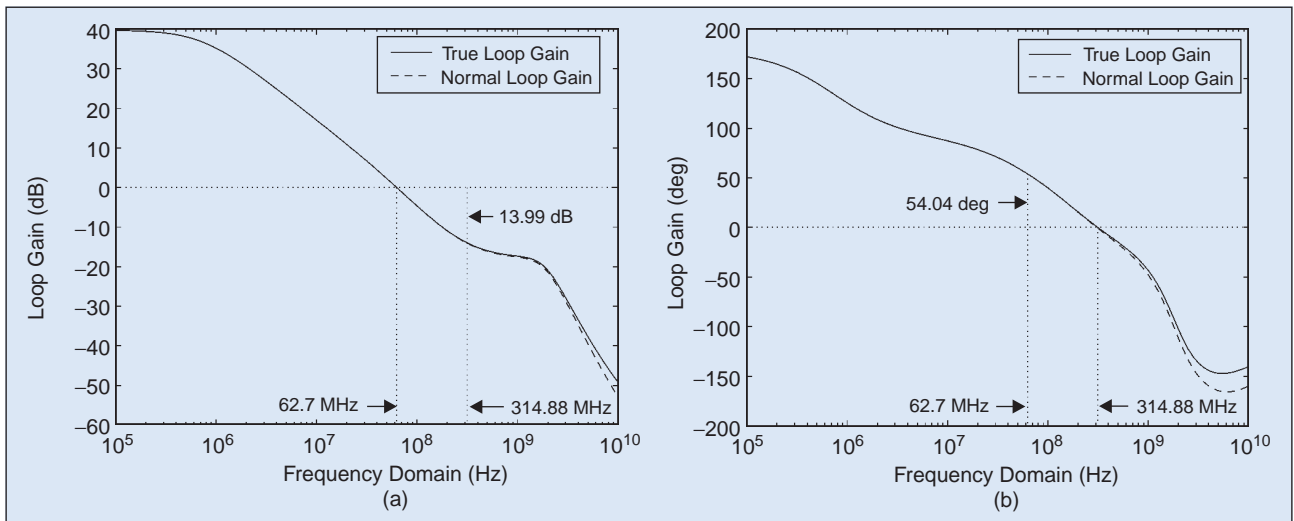
13. The loop gain waveform of the bipolar operational amplifier.

moves higher, the effect of these local loops upon circuit performance cannot be neglected. To conduct the experiment, we first turn off the local return loops by setting the following bsim3v3 model parameters: $xpart = 1$, $capmod = 0$, $cgdo = 0$, $cgdl = 0$, and $cf = 0$. This circuit contains two return loops through R_f and C_f, respectively; however, current probe I_{probe} can be placed as shown in Fig. 10 to break both loops. In addition, there is only one controlled source (g_m of M1) that exists in the network; thus both our loop-based and device-based algorithms produce consistent and accurate loop-gain results as plotted by the solid line in Fig. 11.

Next, we turn back the local return loops by setting the bsim3v3 model parameters as follows: $xpart = 0$, $capmod = 2$, and resetting parameters $cgdo$, $cgdl$, and cf to default such that they are not forced to zero. Due to the existence of local loops, no break point can be found to break all loops; however, there is still only one controlled source (g_m of M1) that exists in the network, and nulling this controlled source actually renders the network to be passive. This corresponds to Case 2 discussed above. Thus,
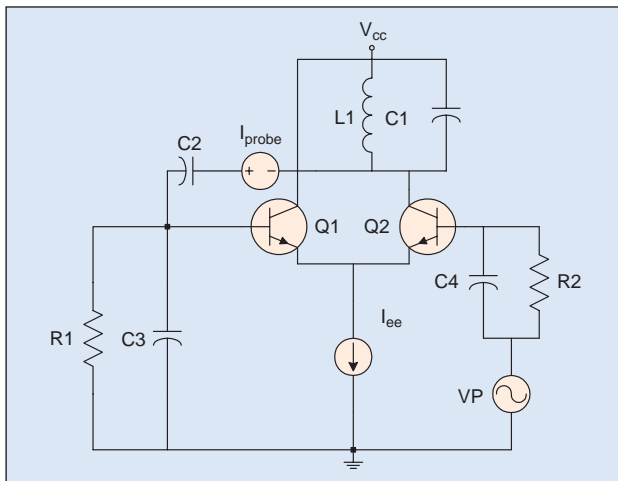
14. An emitter-coupled pair oscillator.
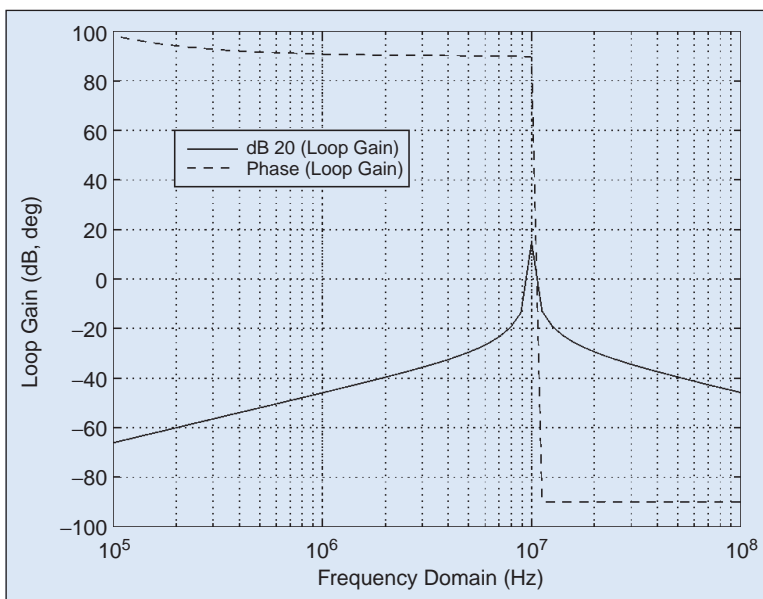
15. Loop gain of the linear oscillator calculated by our loop-based algorithm.

our device-based algorithm still produces accurate loop-gain results as plotted in the dashed line in Fig. 11. Our loop-based algorithm produces results that are inaccurate in high frequencies, (plotted as the dotted line for comparison).

Bipolar Operational Amplifier

Figure 12 shows a bipolar operational amplifier circuit with differential input stage and single feedback loop. This circuit is used to demonstrate the difference between our loop-based algorithm that calculates the true loop gain and Middlebrook's null double-injection technique that calculates the normal loop gain.

Figure 13 plots the loop-gain waveforms produced by our loop-based algorithm and null double-injection technique. It is obvious that the loop-gain waveforms overlapped very well except at high frequency. This difference increases as the frequency goes higher. The reason behind this is that the null double-injection technique only models the normal loop transmission in the return loop, while our loop-based algorithm models both normal and reverse transmission, and the reverse transmission increases as frequency goes higher.

The stability margins can be easily obtained from the loop-gain waveform, and our loop-based algorithm produces gain margin of 13.99 dB at 314.88 MHz and phase margin of 54.04 degree at 62.7 MHz. For a stable circuit or transistor, both gain margin and phase margin should be positive, or the phase plot stays positive within the operating bandwidth. This circuit corresponds to Case 3 discussed above. Nulling the g_m in either Q2 or Q5 does not render the whole network to be passive, and our device-based gain-nulling algorithm does not produce accurate loop-gain results for this circuit.

Linear Oscillator Circuit

Figure 14 shows a linear oscillator circuit referenced from [7]. This circuit is designed to oscillate at a frequency of 10 MHz.

Figure 15 plots both the dB plot and phase plot of loop gain on one graph. The application of stability analysis on the linear oscillator design is to ensure that both the dB plot and phase plot of loop gain are close enough to zero at the desired oscillating frequency and that the phase of loop gain changes rapidly in the neighborhood of the oscillation frequency for good frequency stability.

It is easy to verify from Figure 15 that at 10.6 MHz, the loop gain is 0.04 dB and 1.3 degrees and that the phase of loop gain changes rapidly from 90 degrees to –90 degrees around the oscillating frequency.

Dr. Michael Tian is currently with Cadence Design Systems, where he works on signal integrity and analog and RF CAD. He has previously worked at Lucent Technologies Bell Laboratories and the University of Iowa (e-mail: mtian@cadence.com).

Dr. V. Visvanathan was until recently with Cadence Design Systems. He is currently with Texas Instruments (India) where he works in the ASIC Product Development Center as the Chief Con-

sultant. He has previously worked at Bell Labs and has been on the faculty of the University of Maryland, College Park, and the Indian Institute of Science, Bangalore.

Dr. Jeffrey Hantgan is currently the engineering director for Analog simulation and RF CAD development with Cadence Design Systems, Inc. He has previously worked at AT&T/Lucent Technologies Bell Laboratories and has been on the faculty of The State University of New York at Stony Brook and Cornell University (e-mail: jch@cadence.com).

References

1. H.W. Bode, *Network Analysis and Feedback Amplifier Design.* New York: Van Nostrand, 1945.

2. W.K. Chen, *Active Network and Feedback Amplifier Theory.* New York: McGraw-Hill, and Washington, DC: Hemisphere, 1980, pp. 185-246.

3. P.R. Gray and R.G. Meyer, *Analysis and Design of Analog Integrated Circuits.* 3rd Ed. New York: Wiley, 1993, pp. 535-591.

4. P.J. Hurst, "A comparison of two approaches to feedback circuit analysis," *IEEE Trans. Educ.,* vol. 35, pp. 253-261, Aug. 1992.

5. P.J. Hurst and S.H. Lewis, "Determination of stability using return ratios in balanced fully differential feedback circuits," *IEEE Trans. Circuits Syst. II,* vol. 42, pp. 805-817, Dec. 1995.

6. E.S. Kuh and R.A. Rohrer, *Theory of Linear Active Networks.* San Francisco, CA: Holden-Day, 1967, pp. 520-605.

7. K.S. Kundert, *The Designer's Guide to SPICE and Spectre.* Norwell, MA: Kluwer, 1995, pp. 67-107.

8. D.J.H. Maclean, *Broadband Feedback Amplifiers.* Chichester, NY: Research Studies Press, 1982.

9. R.D. Middlebrook, "Measurement of loop gain in feedback systems," *Int. J. Electronics,* vol. 38, pp. 485-512, Apr. 1975.   CD■

Society News

CAS NAMES NEW EDITOR TO MAGAZINE

Chung-Yu Wu was recently appointed the new CAS editor for *IEEE Circuits & Devices Magazine*, replacing Dr. Mona Zaghloul. Dr. Wu was born in 1950. He received his M.S. and Ph.D. degrees from the Department of Electronics Engineering, National Chiao-Tung University, Taiwan, in 1976 and 1980, respectively.

From 1980 to 1984 he was an associate professor at National Chiao-Tung University. During 1984-1986, he was a visiting associate professor in the Department of Electrical Engineering, Portland State University, Oregon. Since 1987, he has been a professor in the National Chiao- Tung University. He was a recipient of the IEEE Third Millennium Medal; the Outstanding Academic Award by the Ministry of Education in 1999; the Outstanding Research Award by the National Science Council in 1989-90, 1995-96, and 1997-98; the Outstanding Engineering Professor by the Chinese Engineer Association in 1996; and the Tung-Yuan Science and Technology Award in 1997. From 1991 to 1995, he was rotated to serve as director of the Division of Engineering and Applied Science in the National Science Council. Currently, he is the Centennial Honorary Chair Professor at the National Chiao-Tung University.

He has published more than 200 technical papers in international journals and conference proceedings. He also has 18 patents, including nine US patents. Since 1980, he has served as a consultant to high-tech industry and research organizations. He has built up strong research collaborations with high-tech industries. His research interests focus on low-voltage low-power mixed- mode circuits and systems for multimedia applications, hardware implementation of visual and auditory neural systems, RF communication circuits and systems, biochips, and bioelectronics.

Dr. Wu served on the Technical Program Committees of IEEE ISCAS, ICECS, APCCAS. He served as the VLSI Track Co-Chair of the Technical Program Committee of ISCAS'99. He served as a Guest Editor of the Multimedia Special Issue for *IEEE T-CSVT* in August-October 1997. He also served as an associate editor for the *IEEE Transactions on VLSI Systems* and *IEEE Transactions on Circuits and Systems-Part II.* He served as General Chair of IEEE APCCAS'92. Currently, he serves as the associate editor of the *IEEE Transactions on VLSI Systems* and *IEEE Transactions on Multimedia*, and as the Distinguished Lecturer of IEEE CAS Society. He is one of the CAS representatives in the IEEE Neural Network Council and IEEE TAB Nanotechnology Committee. He also serves as the member of the international advisory committee of IEEE APCCAS and ICECS. He is a member of Eta Kappa Nu and Phi Honorary Scholastic societies, and he is a Fellow of IEEE.   CD■